

pubs.acs.org/JACS Article

TetrazineBox: A Structurally Transformative Toolbox

Qing-Hui Guo, Jiawang Zhou, Haochuan Mao, Yunyan Qiu, Minh T. Nguyen, Yuanning Feng, Jiaqi Liang, Dengke Shen, Penghao Li, Zhichang Liu, Michael R. Wasielewski, and J. Fraser Stoddart*



Cite This: J. Am. Chem. Soc. 2020, 142, 5419-5428



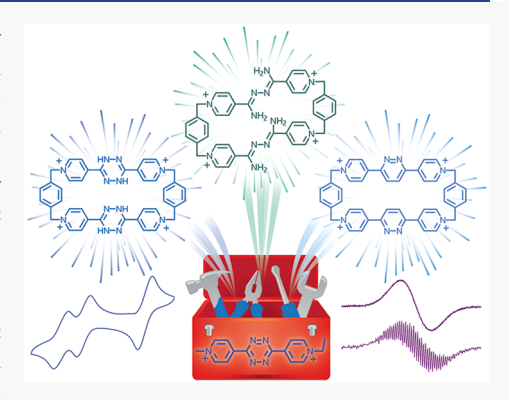
ACCESS

Metrics & More



SI Supporting Information

ABSTRACT: Synthetic macrocycles capable of undergoing allosteric regulation by responding to versatile external stimuli are the subject of increasing attention in supramolecular science. Herein, we report a structurally transformative tetracationic cyclophane containing two 3,6-bis(4-pyridyl)-l,2,4,5-tetrazine (4-bptz) units, which are linked together by two *p*-xylylene bridges. The cyclophane, which possesses modular redox states and structural post-modifications, can undergo two reversibly consecutive two-electron reductions, affording first its bisradical dicationic counterpart, and then subsequently the fully reduced species. Furthermore, one single-parent cyclophane can afford effectively three other new analogs through box-to-box cascade transformations, taking advantage of either reductions or an inverse electron-demand Diels—Alder (IEDDA) reaction. While all four new tetracationic cyclophanes adopt rigid and symmetric box-like conformations, their geometries in relation to size, shape, electronic properties, and binding affinities toward polycyclic



aromatic hydrocarbons can be readily regulated. This structurally transformative tetracationic cyclophane performs a variety of new tasks as a result of structural post-modifications, thus serving as a toolbox for probing the radical properties and generating rapidly a range of structurally diverse cyclophanes by efficient divergent syntheses. This research lays a solid foundation for the introduction of the structurally transformative tetracationic cyclophane into the realm of mechanically interlocked molecules and will provide a toolbox to construct and operate intelligent molecular machines.

■ INTRODUCTION

The design and preparation of functional macrocycles have been key driving forces in promoting major advances in supramolecular chemistry, which was pioneered by Pedersen, Cram,³ and Lehn.⁴ The subsequent decades have witnessed the emergence of plentiful supplies of macrocyclic compounds, including, but not limited to, cyclodextrins, calixarenes, cucurbiturils, expanded porphyrins, pillararenes, and cationic cyclophanes, 10 such as cyclobis (paraquat-p-phenylene) (CBPQT⁴⁺) or the so-called Blue Box. 11 All these macrocycles offered good models for investigating the nature of noncovalent bonding interactions. 12 Meanwhile, they also served as primary building blocks for the construction of advanced (supra)molecular assemblies 6c,7c,13 and functional materials.76,14 In particular, the successful landmarks in synthetic macrocyclic chemistry enabled chemists to construct^{7c,15} artificial molecular machines and investigate 16 the relative motions of their component parts on the molecular scale.

While the properties of these classic macrocycles are well-known, the structural diversity and host—guest chemistry³ of synthetically novel macrocycles continue to be the subjects of investigations¹⁷ in an attempt to unleash new research directions in chemistry and materials science. Typically, most of these synthetic macrocycles, however, are structurally well-defined with rigid stereoelectronic constitutions. Recently, the applications of the so-called post-macrocyclization modifica-

tion and covalent post-assembly modification (PAM) strategies employing synthetic macrocycles containing tetrazine units, which were pioneered by Wang¹⁸ and Nitschke,¹⁹ offered straightforward ways to fabricate complex and functional macrocycles. Here, we report (Scheme 1) a structurally transformative tetrazine-containing tetracationic cyclophane, namely TetrazineBox (TzBox4+), which possesses modular redox states that lead to versatile and modifiable structures. The three reversible redox states of TzBox4+ can be manipulated simply by the application of redox chemistry, and their properties have been revealed fully by cyclic voltammetry (CV), as well as by UV-vis-NIR and EPR spectroscopies. Moreover, TzBox⁴⁺ undergoes box-to-box cascade transformations through either reductions or an inverse electron-demand Diels-Alder (IEDDA) reaction, affording three new cyclophanes. Single-crystal X-ray crystallographic analysis on crystalline samples of these cyclophanes demonstrates that the dimensions of their cavities can be regulated. Finally, as a proof of principle, we show that their

Received: January 29, 2020 Published: February 21, 2020



Scheme 1. Synthesis of the Reference Compound Me₂(4-bptz)·2PF₆ and TzBox·4PF₆

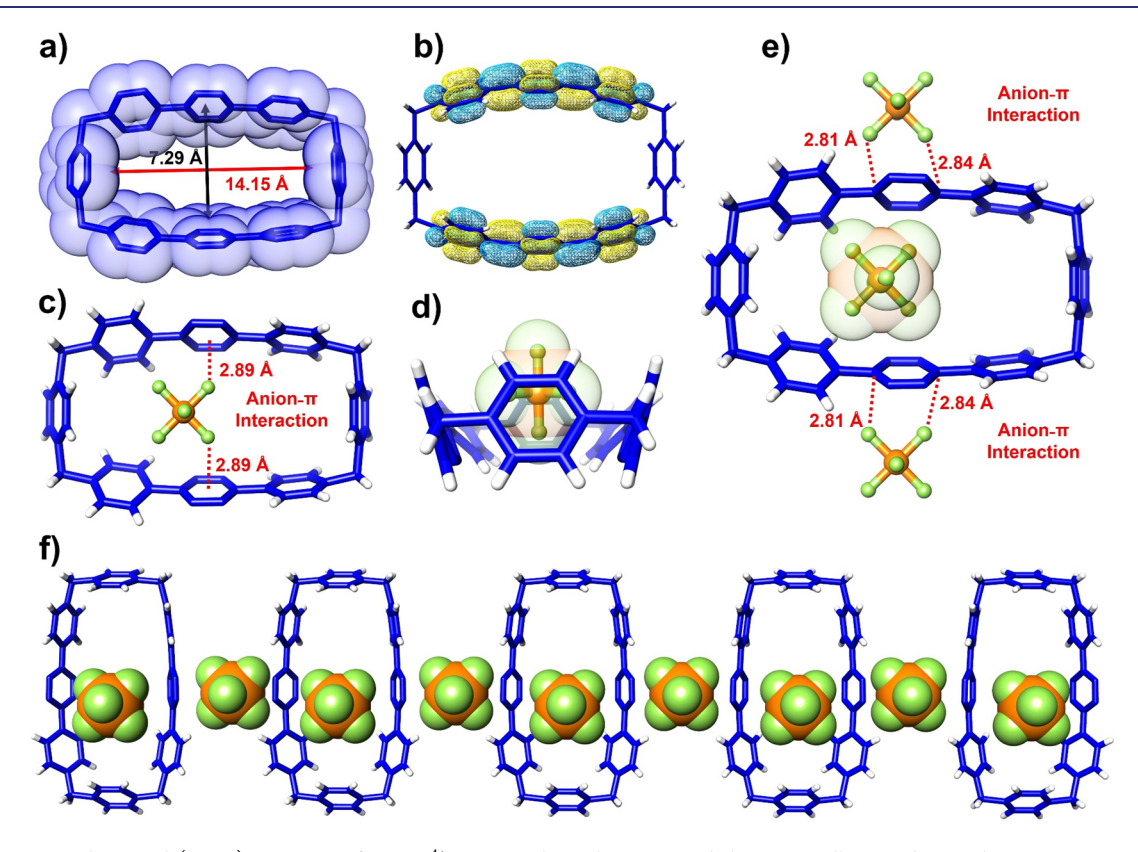


Figure 1. X-ray single-crystal (super)structures of \mathbf{TzBox}^{4+} . Atom colors: the organic skeletons are illustrated as stick representations in blue; P, yellow; F, green. The anion-π interactions are depicted as red dashed lines. (a) Top-down view of \mathbf{TzBox}^{4+} as a stick representation with the corresponding semitransparent space-filling representation superimposed upon it. The dimensions of the cavity are highlighted by black and red arrows. (b) Graphical representation of the DFT-calculated lowest unoccupied molecular orbital (LUMO) of \mathbf{TzBox}^{4+} . (c) A PF₆⁻ counterion located inside the cavity of \mathbf{TzBox}^{4+} as a result of synergistic anion-π interactions. The PF₆⁻ anion is shown as a ball-and-stick representation. (d) Side-on view of the PF₆⁻ counterion situated inside the cavity of \mathbf{TzBox}^{4+} . (e) Anion-π interactions occurring both on the exterior and in the interior of the cavity. The exterior PF₆⁻ counterions are shown as ball-and-stick representations. The interior PF₆⁻ counterion is shown as a ball-and-stick representation with the corresponding semitransparent space-filling representation superimposed upon it. (f) The multiple anion-π interactions assembling \mathbf{TzBox}^{4+} and $\mathbf{PF_6}^-$ counterions into an ordered 1D superstructure. The PF₆⁻ counterions are shown as space-filling representations.

binding affinities toward polycyclic aromatic hydrocarbons (PAHs) can be modulated as a consequence of the variable electronic features of TzBox⁴⁺ and its analogs.

■ RESULTS AND DISCUSSION

Synthesis and Structure of the TetrazineBox. We chose 3,6-bis(4-pyridyl)-l,2,4,5-tetrazine (4-bptz) **1** as a key building block in making **TzBox**⁴⁺ on account of its redox and IEDDA reactions in macrocyclic compounds¹⁸ and coordina-

tion chemistry. ^{19b,21} The incorporation of 4-bptz into a tetracationic cyclophane could be expected to result in a plethora of outcomes. The synthesis of $TzBox\cdot 4PF_6$ is illustrated in Scheme 1. Treatment of 1 with 10 equiv of 1,4-bis(bromomethyl)benzene in $CH_2Cl_2/MeCN$ (1:2), while heating at 90 °C for 18 h, followed by counterion exchange (NH₄PF₆/MeOH), afforded 3·2PF₆ in 70% yield. In the presence of 6 equiv of **pyrene** as a template, with 30 mol% of tetrabutylammonium iodide (TBAI) as a catalyst, the reaction

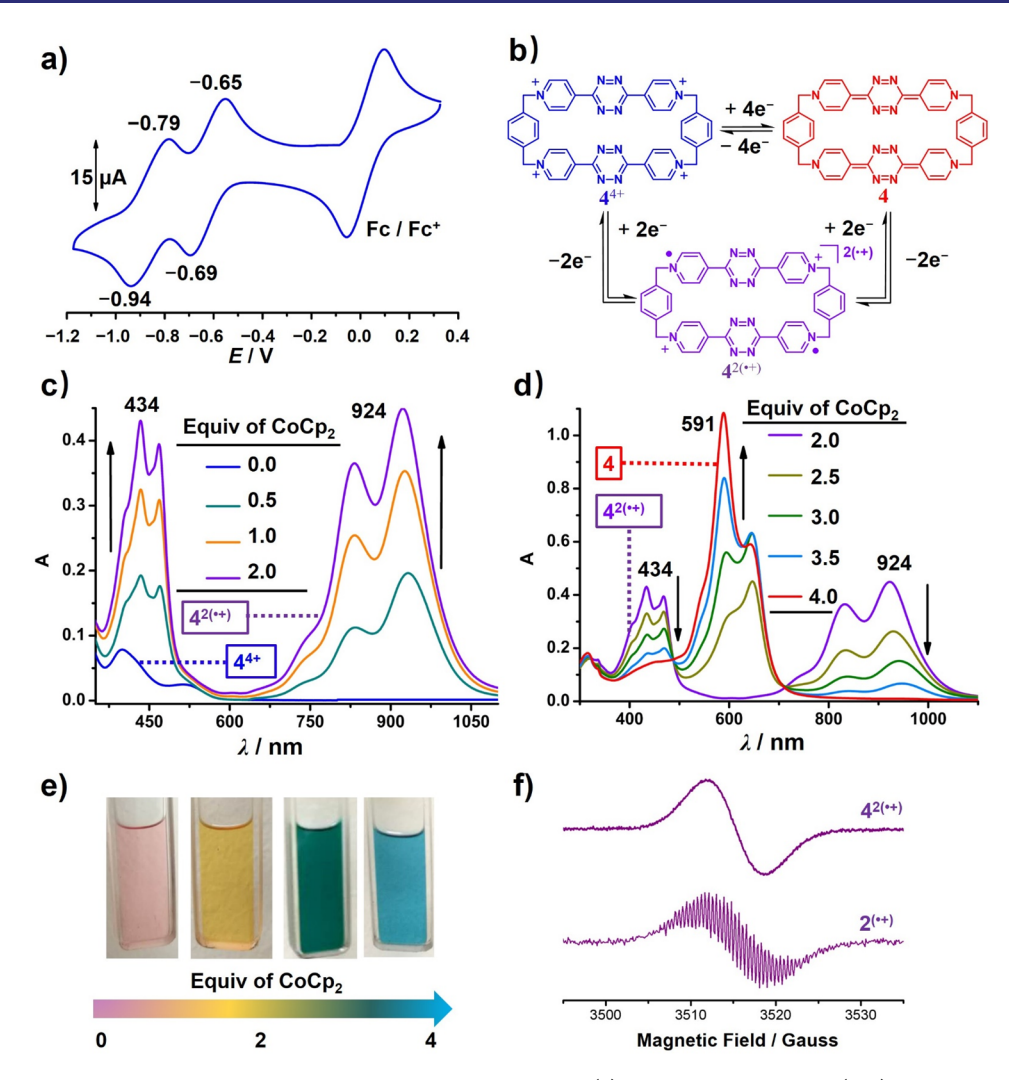


Figure 2. Manipulation and characterization of the redox states of TzBox- $4PF_6$. (a) Cyclic voltammogram (CV) of TzBox- $4PF_6$ recorded (scan rate 100 mV s⁻¹) with a glassy carbon electrode. The experiment was performed at 298 K in an Ar-purged DMF solution (1 mM) with 0.1 M TBAPF₆ as the supporting electrolyte and ferrocene as internal standard. (b) Structural formulas of the three reversible redox state of $TzBox^{4+}$. (c, d) UV-vis-NIR absorption spectra of $TzBox^{4+/2(\bullet+)/0}$, which were obtained by stepwise addition of 0, 0.5, 1.0, 2.0, 2.5, 3.0, 3.5, and 4.0 equiv of CoCp₂. All spectra were recorded in Ar-purged DMF solutions at 298 K. (e) Change of the color of DMF solutions from light pink to yellow to green and finally to blue on stepwise addition of CoCp₂. (f) CW-EPR spectra of $4^{2(\bullet+)}$ and $2^{(\bullet+)}$.

of 3·2PF₆ in MeCN with 4-bptz at 80 °C for 18 h—or at room temperature for 7 days—followed by precipitation of the product with tetrabutylammonium chloride (TBACl), furnished crude **pyrene**⊂**TzBox**·4Cl. The complex, which was subjected to counterion exchange (NH₄PF₆/MeOH), afforded crude **pyrene**⊂**TzBox**·4PF₆. The template (**pyrene**) was removed by reverse-phase column chromatography, and the desired product **TzBox**·4PF₆ was isolated as a red solid in 31% yield. Without the use of **pyrene** as a template in this reaction, the cyclophanes cannot be prepared.

Further atomic-level (super)structural information was obtained (Figure 1) from single-crystal X-ray diffraction (SCXRD) experiments. Orange plate-like single crystals, suitable for SCXRD, were obtained by slow vapor diffusion of *i*Pr₂O into an MeCN solution of **TzBox**·4PF₆ during 1 day. In the solid state, **TzBox**⁴⁺ adopts (Figure 1a) a symmetrical box-like conformation, with average dimensions of 14.1 × 7.3 Å. Density functional theory (DFT) calculations²³ reveal (Figure 1b) that the LUMO of **TzBox**⁴⁺ is highly delocalized on the 4-bptz²⁺ subunits. Superstructural analyses show that

anion- π interactions exist between the $\mathrm{PF_6}^-$ counterions and TzBox⁴⁺. One PF₆⁻ counterion is situated (Figure 1c,d) close to centrosymmetrically inside the cavity of TzBox4+ and interacts synergistically with two 4-bptz²⁺ walls through utilizing anion- π interactions. The distances between the included PF₆⁻ ion and the centroids of the tetrazine units are both 2.89 Å, i.e., well within the typical distances of 2.80-3.50 Å for anion- π interactions recorded in the literature. ^{17d,24} Meanwhile, anion- π interactions also occur (Figure 1e) outside of the box cavity between the two 4-bptz²⁺ units and associated PF_6^- counterions, with distances of 2.81 and 2.84 Å. Finally, multiple anion- π interactions enable the assembly (Figure 1f) of the PF₆⁻ ions and TzBox⁴⁺ into a 1D superstructure. 25 Although similar anion $-\pi$ interactions are also present (Figure S1) in the superstructures of 2.2PF₆, they have never been observed in the solid-state superstructures of other tetracationic cyclophanes, ^{17a} thus highlighting the highly π -electron-deficient nature of the 4-bptz²⁺ units in these two compounds.

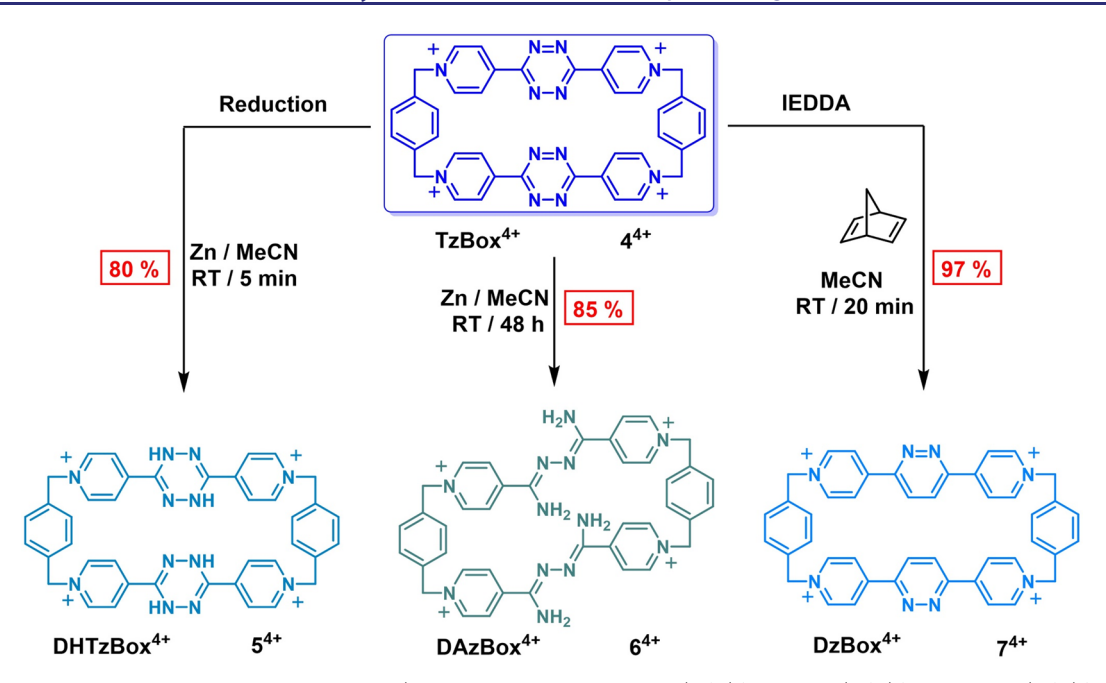


Figure 3. Box-to-box transformations. The parent $TzBox^{4+}$ is transformed to $DHTzBox^{4+}$ (S^{4+}), $DAzBox^{4+}$ (S^{4+}), and $DzBox^{4+}$ (S^{4+}) by reductions and an inverse electron-demand Diels-Alder (IEDDA) reaction.

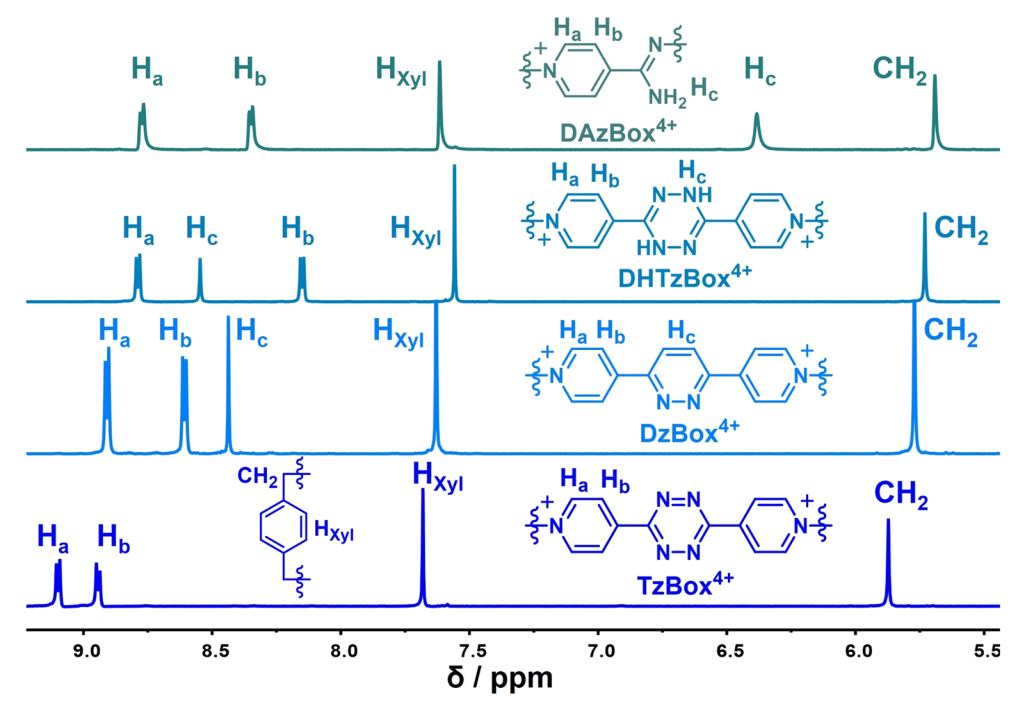


Figure 4. ¹H NMR spectra of DAzBox⁴⁺, DHTzBox⁴⁺, DzBox⁴⁺, and TzBox⁴⁺. All their ¹H NMR spectra recorded in CD₃CN at 298 K reveal single sets of resonances, in keeping with their average molecular symmetry.

Redox Chemistry. Cyclic voltammetry (CV) was performed on $\mathbf{TzBox} \cdot 4PF_6$ and the reference compound $\mathbf{2} \cdot 2PF_6$ in order to shed light on the electrochemical behavior of the rigid cyclophane. $\mathbf{TzBox} \cdot 4PF_6$ consists (Figure 2a) of two well-separated two-electron redox couples, observed at -0.69 and -0.94 V vs Fc/Fc^+ in DMF, corresponding to (Figure 2b) the formation of the bisradical dicationic $\mathbf{TzBox}^{2(\bullet+)}$ and the fully reduced neutral species, \mathbf{TzBox} , respectively. The fact that this transformational process is reversible is supported by the overlapping of the CV curves of 10 repeated cycles. These observations highlight the fact that the three reversible

oxidation states of tetracationic \mathbf{TzBox}^{4+} can be manipulated by simply applying redox chemistry.

In addition, UV-vis-NIR and EPR spectroscopies were used to probe the physicochemical properties of the TzBox⁴⁺ cyclophane and its different redox states in DMF solution by titrating with a one-electron reductant, cobaltocene²⁶ (CoCp₂), under an Ar atmosphere. Upon stepwise addition of CoCp₂ to a solution of TzBox·4PF₆, the characteristic absorbances (Figure 2c) of the bisradical dicationic TzBox^{2(*+)}, i.e., two sets of absorption bands at around 434 and 924 nm, increase in their intensities gradually in the

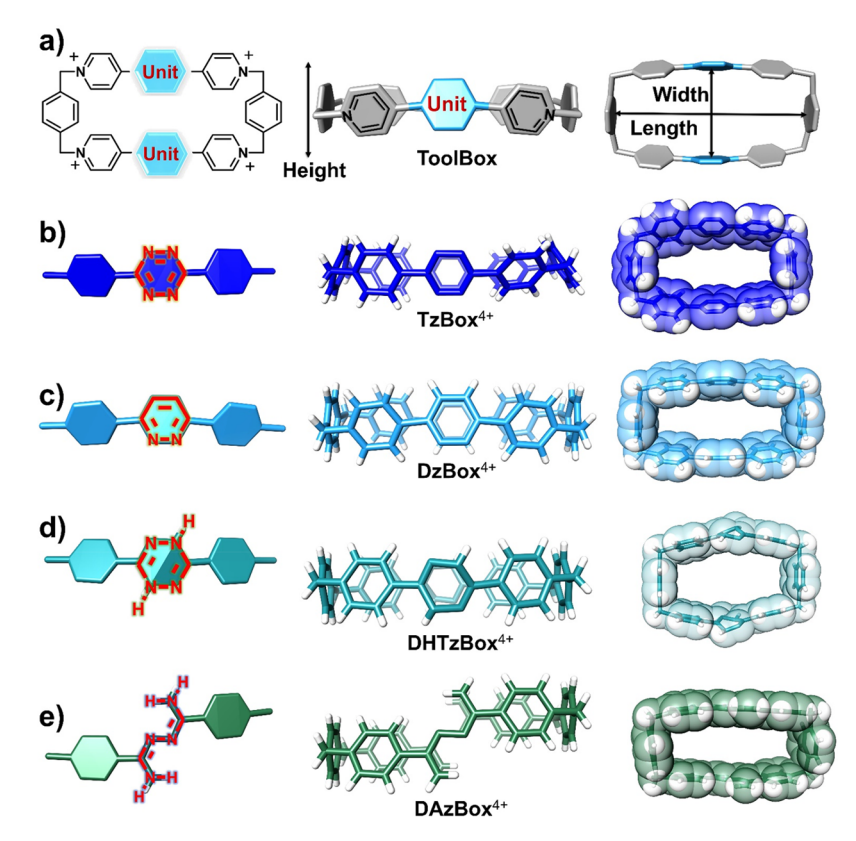


Figure 5. Illustration of box cavities the of tetracationic cyclophane analogs in solid state. (a) Schematic diagrams showing the box-like conformations and the dimensions of the cavities, related to their heights, widths, and lengths. Different representations of the single-crystal structures of (b)TzBox⁴⁺, (c) DzBox⁴⁺, (d) DHTzBox⁴⁺, and (e) DAzBox⁴⁺. Left, graphical representations of the structures of the spacers. Middle, stick representations of box-like cavities. Right, stick representations with the corresponding semitransparent space-filling representations superimposed upon them.

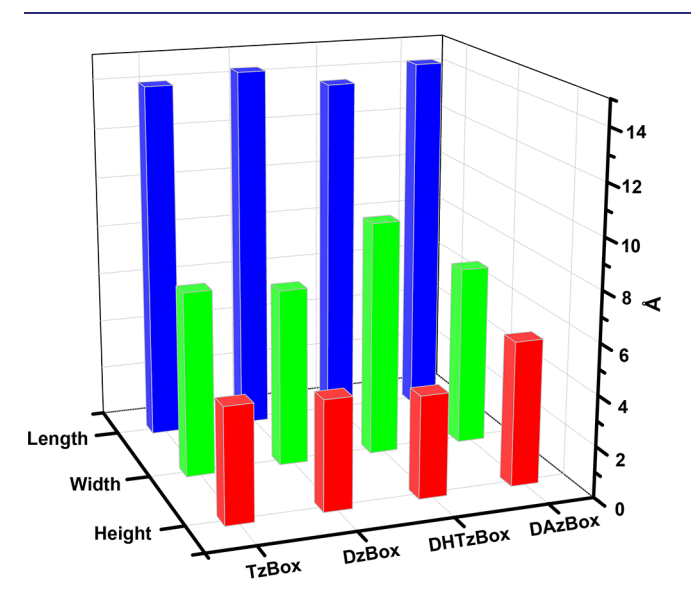


Figure 6. Histogram comparing the cavities in **TzBox**⁴⁺, **DzBox**⁴⁺, **DHTzBox**⁴⁺, and **DAzBox**⁴⁺ in relation to the dimensions of heights, widths, and lengths.

spectrum. The **TzBox**⁴⁺ was converted quantitatively to the bisradical dication **TzBox**^{2(•+)} on addition of 2 equiv of CoCp₂. When more than 2 equiv of the reductant were added, the intensities of the bands around at 434 and 924 nm both decreased (Figure 2d), while a new adsorption band centered at 591 nm appeared. This new band, which was attributed to

the formation of the fully reduced cyclophane **TzBox** in quantitative yield by employing 4 equiv of CoCp₂, was evidenced by the concomitant disappearance of the absorption bands of the bisradical dications and the maximal absorption intensity of the band at around 591 nm. The continuous shifts of the absorption bands are exactly in line with the heterochromatic changes (Figure 2e) of the solutions. The colors of the solutions changed from light pink to yellow to green and then finally to blue. Furthermore, **TzBox**^{2(•+)} and **TzBox** can also be obtained (Figure S22) by reducing **TzBox**⁴⁺ with Zn powder in Ar-purged dry MeCN and DMF solutions, respectively.

Continuous-wave EPR spectra provide (Figure 2f) further evidence for the formation of radical cations. The spectrum of reference compound $2\cdot 2PF_6$ exhibits multiple peaks as a result of the hyperfine splitting from the protons and nitrogen, an observation which is consistent with the EPR signal reported in the literature. The EPR spectrum of $TzBox^{2(\bullet+)}$ shows a complete absence of hyperfine structure, most likely because of intramolecular spin-exchange interactions between the unpaired electrons from the dimeric 4-bptz^(\bullet+) units, which are isolated about 7 Å apart as a result of bridging by a pair of p-xylylene linkers.

Box-to-Box Transformations. The facile and reversible redox chemistry of $TzBox^{4+}$ encouraged us to grow single crystals of the bisradical dicationic $TzBox^{2(\bullet+)}$ and the neutral TzBox. Unexpectedly, reducing $TzBox^{4+}$ in a glovebox with an excess of Zn powder for 5 min and 48 h, respectively, led to (Figure 3) two different products, namely, **Dihydro-tetrazine-**

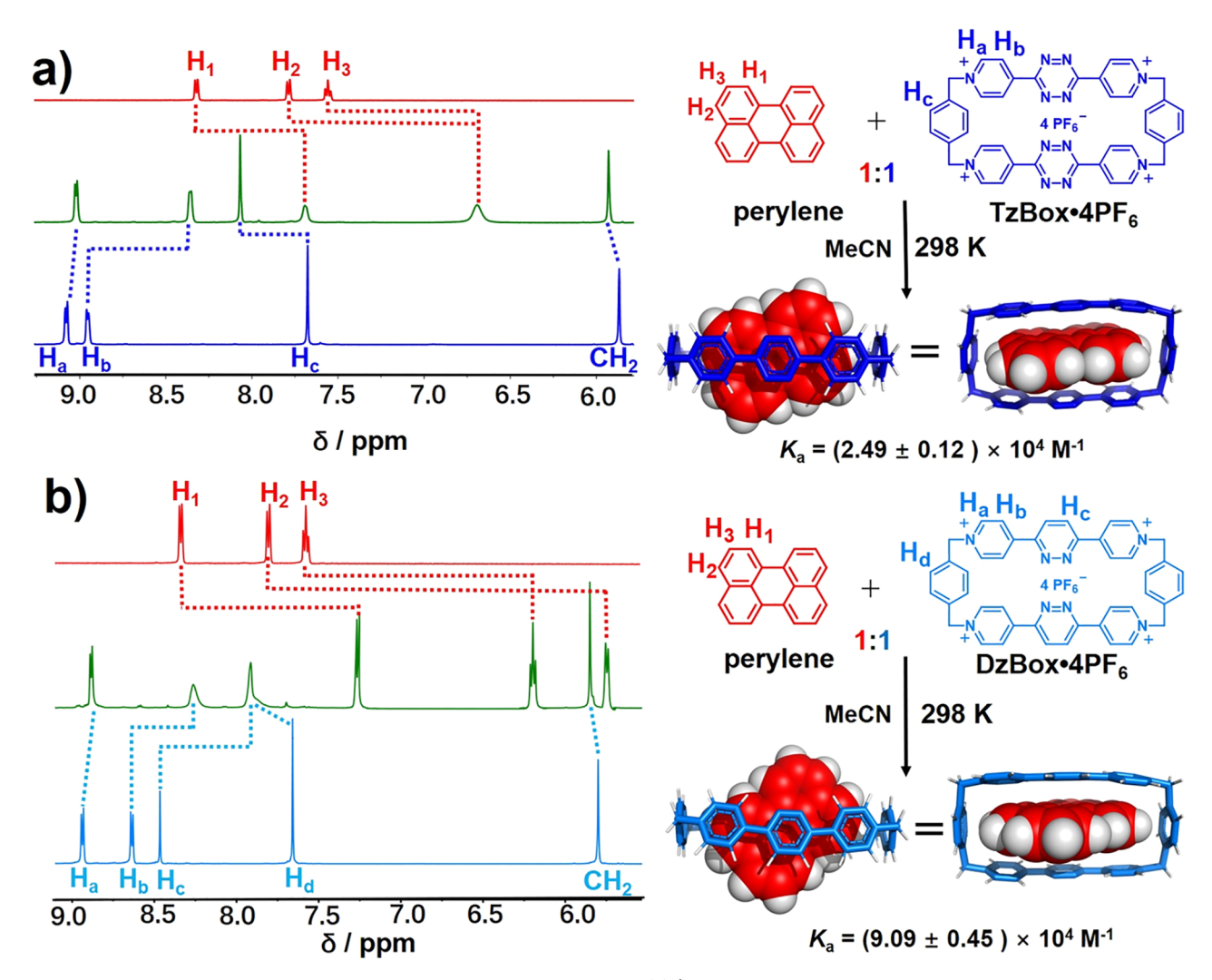


Figure 7. Binding affinities of $TzBox \cdot 4PF_6$ and $DzBox \cdot 4PF_6$ toward perylene. (a) ¹H NMR spectra of perylene, $TzBox \cdot 4PF_6$, and their 1:1 mixture recorded in CD_3CN solution as well as the single-crystal structure of the inclusion complex. The perylene is highlighted as a space-filling representation in red. The organic skeleton of $TzBox^{4+}$ is illustrated as a stick representation in blue. (b) ¹H NMR spectra of perylene, $DzBox^{4+}$ 4PF₆, and their 1:1 mixture in CD_3CN solution as well as the single-crystal superstructure of the inclusion complex. The perylene is highlighted as a space-filling representation in red. The organic skeleton of $DzBox^{4+}$ is illustrated as a stick representation in light blue.

Box (DHTzBox⁴⁺) and DiaminoazineBox (DAzBox⁴⁺). We speculate that both $TzBox^{2(\bullet+)}$ and TzBox are extremely reactive and sensitive toward protons, oxygen, and other electrophiles in solution. In the presence of Zn powder and a small amount of H₂O in MeCN, a reductive hydrogenation involving two consecutive single-electron reductions, followed by protonation, transforms (Scheme S7a) the aromatic tetrazine into the nonplanar 1,4-dihydro-tetrazine, producing DHTzBox⁴⁺. On prolonging the reduction time (48 h), a ringopening reaction subsequently converts 1,4-dihydro-tetrazine to the acyclic product, diaminoazine. The intermediate **DHTzBox**⁴⁺ was converted finally to **DAzBox**⁴⁺. While reducing tetrazine has been reported²⁹ in metal-coordination chemistry literature, to the best of our knowledge, the structures presented here are the first examples of exploring both reactions in the context of organic molecules. The mechanisms of the reductions and box-to-box transformations are summarized in Scheme S7. In comparison with the traditional stepwise syntheses of macrocycles, this box-to-box transformation, not only demonstrates the versatile nature of the parent macrocycle, but also enables us to introduce various

functional groups—such as a secondary amino group into **DHTzBox**⁴⁺ and a primary amino group into **DAzBox**⁴⁺—that would otherwise be incompatible with the conditions of forming the parent **TzBox**⁴⁺. In order to expand the scope of the box-to-box transformation, the preparation³⁰ of **Diazine-Box** (**DzBox**⁴⁺) in 97% yield employing an IEDDA reaction was also demonstrated. All these tetracationic cyclophane analogs were fully characterized by recording their ¹H and ¹³C NMR spectra (Figures S12–S21) in addition to their high-resolution mass spectra. All the ¹H NMR spectra reveal (Figure 4) single sets of resonances on account of their symmetric conformations in solution.

Regulatable Cavities and Binding Affinities. X-ray crystallography reveals unambiguously the conformations of the cyclophane analogs in the solid state. Ignoring the influence of the spacers between the pyridinium units, all these analogs adopt (Figure 5) a box-like geometry. The dimensions of the cavities of these tetracationic cyclophanes, related to (Figures 5 and 6, and Table S1) their heights, widths, and lengths, ³¹ are regulatable. TzBox⁴⁺ and DzBox⁴⁺ share similar shapes with ca. 4.4, 7.1, and 14.3 Å characterizing

their heights, widths, and lengths, respectively, since the spacers in these two boxes are both rigid six-membered aromatic rings, namely tetrazine and diazine. The characteristic curve-shape of **DHTzBox**⁴⁺ has the smallest height and length, while possessing the largest width as a consequence of its flexible spacers, namely dihydro-tetrazine. The largest height of **DAzBox**⁴⁺, accompanied by average values of width and length, is attributed to the relaxed conformation of the spacer with ring-opening structures.

These regulatable geometries of progenitor and analogs hold out the prospect of modulating their binding abilities toward a myriad of guests. In order to give some substance to this hypothesis, we chose³² TzBox·4PF₆ and DzBox·4PF₆ to probe their binding abilities toward both pyrene and perylene. The dramatic shifts in the proton resonances in the ¹H NMR spectra associated with the hosts, guests and mixtures indicate (Figure 7) the formation of inclusion complexes. In addition, all the 1:1 host-guest mixtures show (Figures S4-S7) characteristic charge-transfer (CT) bands in the UV-vis absorption spectra. Job's plots confirm (Figures S4-S7) their 1:1 stoichiometries. On the basis of the UV-vis titration data, the binding constants (K_a) were calculated (Figure 7 and Figures S4-S7) to be $(1.54 \pm 0.08) \times 10^4$ (pyrene \subset TzBox⁴⁺), $(2.49 \pm 0.12) \times 10^4$ (perylene \subset TzBox⁴⁺), $(1.62 \pm 0.08) \times$ 10^4 (pyrene \subset DzBox⁴⁺), and (9.09 \pm 0.45) \times 10⁴ M⁻¹ (perylene⊂DzBox⁴⁺). Both TzBox·4PF₆ and DzBox·4PF₆ exhibit similar and weak binding affinities toward pyrene because of the mismatched sizes of the hosts and guests, while their binding affinities toward perylene are quite different. The binding constant between DzBox⁴⁺ and perylene is almost 5 times larger than that between TzBox4+ and perylene. The difference in binding constants can be ascribed to the different electronic properties present in TzBox⁴⁺ and DzBox⁴⁺. CV and differential pulse voltammetry (DPV) show (Figure S8) the more positive reduction potentials of TzBox4+, revealing its more electron-deficient environment which is favorable for the inclusion of PF_6^- ions in the cavity as a result of anion- π interactions, as also evidenced in the single crystal structure of TzBox·4PF₆. The presence of PF₆⁻ ions, however, prevents guests from entering the cavity, resulting in an inferior association constant.3

Concrete evidence for the formation of 1:1 inclusion complexes and their binding models are evaluated from their solid-state superstructures. The X-ray superstructural analysis reveals (Figure S9) that the guests sit inside the cavity of the hosts in order to achieve the maximum face-to-face π -surface overlaps. The stacking distances between the guests and the tetracationic cyclophanes are ca. 3.5 Å, a typical distance for strong $[\pi \cdots \pi]$ interactions. In comparison with **pyrene**, **perylene** has a larger π surface which is more favorable for inclusion in the cavities of \mathbf{TzBox}^{4+} and \mathbf{DzBox}^{4+} . Moreover, this larger size also enhances the $[C-H\cdots \pi]$ interactions in the complexes, an observation which is reflected by the shorter distances between the protons of the guests and the π surfaces of p-xylylene units.

CONCLUSIONS

In summary, a structurally transformative tetracationic cyclophane has been designed and synthesized. The cyclophane exists in three different reversible redox states which can be manipulated and visited by delicately controlled redox chemistry. The parent cyclophane can also be transformed into three new cyclophane analogs by use of efficient box-to-

box transformations. All four tetracationic cyclophanes adopt rigid box-like conformations. Their cavity geometries, electronic properties, and binding abilities toward PAHs, are regulatable. Our investigation demonstrates that one specially designed tetracationic cyclophane can perform a variety of tasks, thus serving as a toolbox for probing the radical chemistry and generating libraries of analogs with more intricate box-like structures. The incorporation of such a structurally transformative tetracationic cyclophane into mechanically interlocked molecules will provide a way of controlling and manipulating the behavior of artificial molecular machines.

ASSOCIATED CONTENT

Supporting Information

The Supporting Information is available free of charge at https://pubs.acs.org/doi/10.1021/jacs.0c01114.

Detailed information regarding the experimental methods and procedures, X-ray crystallographic data, and supporting figures and tables (PDF)

X-ray crystallographic data for 4·PF₆ (CIF)

X-ray crystallographic data for 5-PF₆ (CIF)

X-ray crystallographic data for 2·PF₆ (CIF)

X-ray crystallographic data for 6·PF₆ (CIF)

X-ray crystallographic data for 7-PF₆ (CIF)

X-ray crystallographic data for 4-pyrene (CIF)

X-ray crystallographic data for 4-perylene (CIF)

X-ray crystallographic data for 7-pyrene (CIF)

X-ray crystallographic data for 7-perylene (CIF)

AUTHOR INFORMATION

Corresponding Author

J. Fraser Stoddart — Department of Chemistry, Northwestern University, Evanston, Illinois 60208, United States; Institute for Molecular Design and Synthesis, Tianjin University, Tianjin 300072, China; School of Chemistry, University of New South Wales, Sydney, NSW 2052, Australia; orcid.org/0000-0003-3161-3697; Email: stoddart@northwestern.edu

Authors

Qing-Hui Guo — Department of Chemistry, Northwestern University, Evanston, Illinois 60208, United States;
occid.org/0000-0002-9946-0810

Jiawang Zhou — Department of Chemistry and Institute for Sustainability and Energy at Northwestern, Northwestern University, Evanston, Illinois 60208, United States;

occid.org/0000-0002-2399-0030

Haochuan Mao – Department of Chemistry and Institute for Sustainability and Energy at Northwestern, Northwestern University, Evanston, Illinois 60208, United States

Yunyan Qiu — Department of Chemistry, Northwestern University, Evanston, Illinois 60208, United States; orcid.org/0000-0001-9279-4714

Minh T. Nguyen – Department of Chemistry, Northwestern University, Evanston, Illinois 60208, United States; orcid.org/0000-0002-9043-9580

Yuanning Feng — Department of Chemistry, Northwestern University, Evanston, Illinois 60208, United States

Jiaqi Liang — Department of Chemistry, Northwestern University, Evanston, Illinois 60208, United States

Dengke Shen – Department of Chemistry, Northwestern University, Evanston, Illinois 60208, United States

- Penghao Li Department of Chemistry, Northwestern University, Evanston, Illinois 60208, United States;
 orcid.org/0000-0002-1517-5845
- Zhichang Liu School of Science, Westlake University, Hangzhou 310024, China; ⊙ orcid.org/0000-0003-3412-512X

Michael R. Wasielewski — Department of Chemistry and Institute for Sustainability and Energy at Northwestern, Northwestern University, Evanston, Illinois 60208, United States: orcid.org/0000-0003-2920-5440

Complete contact information is available at: https://pubs.acs.org/10.1021/jacs.0c01114

Notes

The authors declare no competing financial interest.

■ ACKNOWLEDGMENTS

The authors thank Northwestern University for financial support. This work was supported by the National Science Foundation under grant CHE-1900422 (M.R.W.). We thank the Integrated Molecular Structure Education and Research Center (IMSERC) for allowing us make use of the facilities. Z.L. acknowledges the support to the National Natural Science Foundation of China (No. 21971211) and the Supercomputer Center of Westlake University.

■ REFERENCES

- (1) (a) Beer, P. D.; Gale, P. A.; Smith, D. K. Supramolecular Chemistry; Oxford University Press, 1999. (b) Steed, J. W.; Atwood, J. L. Supramolecular Chemistry; Wiley, 2013. (c) Liu, Z.; Nalluri, S. K. M.; Stoddart, J. F. Surveying Macrocyclic Chemistry: From Flexible Crown Ethers to Rigid Cyclophanes. Chem. Soc. Rev. 2017, 46, 2459—2478.
- (2) Pedersen, C. J. The Discovery of Crown Ethers. Angew. Chem., Int. Ed. Engl. 1988, 27, 1021–1027.
- (3) Cram, D. J. The Design of Molecular Hosts, Guests, and Their Complexes. *Angew. Chem., Int. Ed. Engl.* **1988**, 27, 1009–1020.
- (4) Lehn, J.-M. Supramolecular Chemistry—Scope and Perspectives Molecules, Supermolecules, and Molecular Devices. *Angew. Chem., Int. Ed. Engl.* 1988, 27, 89–112.
- (5) Cyclodextrins have been investigated since the beginning of the 20th century. See: (a) Stoddart, J. F. A Century of Cyclodextrins. Carbohydr. Res. 1989, 192, R12–R15. (b) Dodziuk, H. Cyclodextrins and Their Complexes: Chemistry, Analytical Methods, Applications; Wiley, 2006. (c) Szejtli, J. Introduction and General Overview of Cyclodextrin Chemistry. Chem. Rev. 1998, 98, 1743–1754.
- (6) (a) Gutsche, C. D.; Dhawan, B.; No, K. H.; Muthukrishnan, R. Calixarenes. 4. The Synthesis, Characterization, and Properties of the Calixarenes from *p-tert*-Butylphenol. *J. Am. Chem. Soc.* **1981**, *103*, 3782–3792. (b) Gutsche, C. D. Calixarenes. *Acc. Chem. Res.* **1983**, *16*, 161–170. (c) Ikeda, A.; Shinkai, S. Novel Cavity Design Using Calix[n]arene Skeletons: Toward Molecular Recognition and Metal Binding. *Chem. Rev.* **1997**, *97*, 1713–1734. (d) Shinkai, S. Calixarenes— the Third Generation of Supramolecules. *Tetrahedron* **1993**, *49*, 8933–8968.
- (7) (a) Freeman, W. A.; Mock, W. L.; Shih, N. Y. Cucurbituril. J. Am. Chem. Soc. 1981, 103, 7367–7368. (b) Kim, J.; Jung, I.-S.; Kim, S.-Y.; Lee, E.; Kang, J.-K.; Sakamoto, S.; Yamaguchi, K.; Kim, K. New Cucurbituril Homologues: Syntheses, Isolation, Characterization, and X-Ray Crystal Structures of Cucurbit[n]uril (N= 5, 7, and 8). J. Am. Chem. Soc. 2000, 122, 540–541. (c) Kim, K. Mechanically Interlocked Molecules Incorporating Cucurbituril and Their Supramolecular Assemblies. Chem. Soc. Rev. 2002, 31, 96–107. (d) Lee, J. W.; Samal, S.; Selvapalam, N.; Kim, H. J.; Kim, K. Cucurbituril Homologues and Derivatives: New Opportunities in Supramolecular Chemistry. Acc. Chem. Res. 2003, 36, 621–630. (e) Lagona, J.;

- Mukhopadhyay, P.; Chakrabarti, S.; Isaacs, L. The Cucurbit[n]uril Family. Angew. Chem., Int. Ed. 2005, 44, 4844–4870. (f) Kim, K.; Selvapalam, N.; Ko, Y. H.; Park, K. M.; Kim, D.; Kim, J. Functionalized Cucurbiturils and Their Applications. Chem. Soc. Rev. 2007, 36, 267–279. (g) Isaacs, L. Cucurbit[n]urils: From Mechanism to Structure and Function. Chem. Commun. 2009, 619–629.
- (8) (a) Sessler, J. L.; Seidel, D. Synthetic Expanded Porphyrin Chemistry. *Angew. Chem., Int. Ed.* **2003**, *42*, 5134–5175. (b) Saito, S.; Osuka, A. Expanded Porphyrins: Intriguing Structures, Electronic Properties, and Reactivities. *Angew. Chem., Int. Ed.* **2011**, *50*, 4342–4373. (c) O'Sullivan, M. C.; Sprafke, J. K.; Kondratuk, D. V.; Rinfray, C.; Claridge, T. D.; Saywell, A.; Blunt, M. O.; O'Shea, J. N.; Beton, P. H.; Malfois, M.; Anderson, H. L. Vernier Templating and Synthesis of a 12-Porphyrin Nano-Ring. *Nature* **2011**, *469*, 72–75.
- (9) (a) Ogoshi, T.; Kanai, S.; Fujinami, S.; Yamagishi, T. A.; Nakamoto, Y. Para-Bridged Symmetrical Pillar[5]arenes: Their Lewis Acid Catalyzed Synthesis and Host-Guest Property. J. Am. Chem. Soc. 2008, 130, 5022–5023. (b) Cao, D.; Kou, Y.; Liang, J.; Chen, Z.; Wang, L.; Meier, H. A Facile and Efficient Preparation of Pillararenes and a Pillarquinone. Angew. Chem., Int. Ed. 2009, 48, 9721–9723. (c) Cragg, P. J.; Sharma, K. Pillar[5]arenes: Fascinating Cyclophanes with a Bright Future. Chem. Soc. Rev. 2012, 41, 597–607. (d) Xue, M.; Yang, Y.; Chi, X.; Zhang, Z.; Huang, F. Pillararenes, a New Class of Macrocycles for Supramolecular Chemistry. Acc. Chem. Res. 2012, 45, 1294–1308.
- (10) Dale, E. J.; Vermeulen, N. A.; Juricek, M.; Barnes, J. C.; Young, R. M.; Wasielewski, M. R.; Stoddart, J. F. Supramolecular Explorations: Exhibiting the Extent of Extended Cationic Cyclophanes. *Acc. Chem. Res.* **2016**, *49*, 262–273.
- (11) Odell, B.; Reddington, M. V.; Slawin, A. M. Z.; Spencer, N.; Stoddart, J. F.; Williams, D. J. Cyclobis (Paraquat-*p*-Phenylene). A Tetracationic Multipurpose Receptor. *Angew. Chem., Int. Ed. Engl.* **1988**, *27*, 1547–1550.
- (12) (a) Lee, T.-C.; Kalenius, E.; Lazar, A. I.; Assaf, K. I.; Kuhnert, N.; Grün, C. H.; Jänis, J.; Scherman, O. A.; Nau, W. M. Chemistry inside Molecular Containers in the Gas Phase. *Nat. Chem.* **2013**, *5*, 376–382. (b) Wang, D.-X.; Zheng, Q.-Y.; Wang, Q.-Q.; Wang, M.-X. Halide Recognition by Tetraoxacalix[2]arene[2]triazine Receptors: Concurrent Noncovalent Halide- π and Lone-Pair- π Interactions in Host-Halide-Water Ternary Complexes. *Angew. Chem., Int. Ed.* **2008**, 47, 7485–7488. (c) Wang, D.-X.; Wang, M.-X. Anion- π Interactions: Generality, Binding Strength, and Structure. *J. Am. Chem. Soc.* **2013**, 135, 892–897.
- (13) (a) Harada, A.; Li, J.; Kamachi, M. The Molecular Necklace: A Rotaxane Containing Many Threaded α -Cyclodextrins. *Nature* **1992**, 356, 325–327. (b) Nepogodiev, S. A.; Stoddart, J. F. Cyclodextrin-Based Catenanes and Rotaxanes. *Chem. Rev.* **1998**, 98, 1959–1976. (c) Harada, A. Cyclodextrin-Based Molecular Machines. *Acc. Chem. Res.* **2001**, 34, 456–464. (d) Liu, Y.; Yu, Y.; Gao, J.; Wang, Z.; Zhang, X. Water-Soluble Supramolecular Polymerization Driven by Multiple Host-Stabilized Charge-Transfer Interactions. *Angew. Chem., Int. Ed.* **2010**, 49, 6576–6579.
- (14) (a) Bew, S. P.; Burrows, A. D.; Duren, T.; Mahon, M. F.; Moghadam, P. Z.; Sebestyen, V. M.; Thurston, S. Calix[4]arene-Based Metal-Organic Frameworks: Towards Hierarchically Porous Materials. Chem. Commun. 2012, 48, 4824–4826. (b) Hu, Q. D.; Tang, G. P.; Chu, P. K. Cyclodextrin-Based Host-Guest Supramolecular Nanoparticles for Delivery: From Design to Applications. Acc. Chem. Res. 2014, 47, 2017–2025. (c) Qi, Z.; Schalley, C. A. Exploring Macrocycles in Functional Supramolecular Gels: From Stimuli Responsiveness to Systems Chemistry. Acc. Chem. Res. 2014, 47, 2222–2233. (d) Harada, A.; Takashima, Y.; Nakahata, M. Supramolecular Polymeric Materials via Cyclodextrin-Guest Interactions. Acc. Chem. Res. 2014, 47, 2128–2140. (e) Hu, X. Y.; Xiao, T.; Lin, C.; Huang, F.; Wang, L. Dynamic Supramolecular Complexes Constructed by Orthogonal Self-Assembly. Acc. Chem. Res. 2014, 47, 2041–2051.

- (15) (a) Langton, M. J.; Beer, P. D. Rotaxane and Catenane Host Structures for Sensing Charged Guest Species. *Acc. Chem. Res.* **2014**, 47, 1935–1949. (b) Bruns, C. J.; Stoddart, J. F. Rotaxane-Based Molecular Muscles. *Acc. Chem. Res.* **2014**, 47, 2186–2199. (c) Stoddart, J. F. The Chemistry of the Mechanical Bond. *Chem. Soc. Rev.* **2009**, 38, 1802–1820. (d) Bruns, C. J.; Stoddart, J. F. *The Nature of the Mechanical Bond: From Molecules to Machines*; Wiley, 2016
- (16) (a) Stoddart, J. F. Mechanically Interlocked Molecules (MIMs)—Molecular Shuttles, Switches, and Machines (Nobel Lecture). Angew. Chem., Int. Ed. 2017, 56, 11094–11125. (b) Sauvage, J.-P. From Chemical Topology to Molecular Machines (Nobel Lecture). Angew. Chem., Int. Ed. 2017, 56, 11080–11093.
- (17) (a) Barnes, J. C.; Juríček, M.; Strutt, N. L.; Frasconi, M.; Sampath, S.; Giesener, M. A.; McGrier, P. L.; Bruns, C. J.; Stern, C. L.; Sarjeant, A. A.; Stoddart, J. F. ExBox: A Polycyclic Aromatic Hydrocarbon Scavenger. J. Am. Chem. Soc. 2013, 135, 183-192. (b) Juríček, M.; Barnes, J. C.; Dale, E. J.; Liu, W. G.; Strutt, N. L.; Bruns, C. J.; Vermeulen, N. A.; Ghooray, K. C.; Sarjeant, A. A.; Stern, C. L.; Botros, Y. Y.; Goddard, W. A., III; Stoddart, J. F. Ex²Box: Interdependent Modes of Binding in a Two-Nanometer-Long Synthetic Receptor. J. Am. Chem. Soc. 2013, 135, 12736-12746. (c) Wang, M.-X. Nitrogen and Oxygen Bridged Calixaromatics: Synthesis, Structure, Functionalization, and Molecular Recognition. Acc. Chem. Res. 2012, 45, 182-195. (d) Guo, Q.-H.; Fu, Z.-D.; Zhao, L.; Wang, M.-X. Synthesis, Structure, and Properties of O₆-Corona[3]arene[3]tetrazines. Angew. Chem., Int. Ed. 2014, 53, 13548-13552. (e) Liu, Y.; Zhao, W.; Chen, C. H.; Flood, A. H. Chloride Capture Using a C-H Hydrogen-Bonding Cage. Science 2019, 365, 159-161. (f) Liu, Y.; Sengupta, A.; Raghavachari, K.; Flood, A. H. Anion Binding in Solution: Beyond the Electrostatic Regime. Chem. 2017, 3, 411-427. (g) Wu, J. R.; Yang, Y. W. Geminiarene: Molecular Scale Dual Selectivity for Chlorobenzene and Chlorocyclohexane Fractionation. J. Am. Chem. Soc. 2019, 141, 12280-12287. (h) Jie, K.; Zhou, Y.; Li, E.; Huang, F. Nonporous Adaptive Crystals of Pillararenes. Acc. Chem. Res. 2018, 51, 2064-2072. (i) Ke, H.; Yang, L. P.; Xie, M.; Chen, Z.; Yao, H.; Jiang, W. Shear-Induced Assembly of a Transient yet Highly Stretchable Hydrogel Based on Pseudopolyrotaxanes. Nat. Chem. 2019, 11, 470-477. (j) Li, B.; Wang, B.; Huang, X.; Dai, L.; Cui, L.; Li, J.; Jia, X.; Li, C. Terphen[n]arenes and Quaterphen[n]arenes (N = 3-6): One-Pot Synthesis, Self-Assembly into Supramolecular Gels, and Iodine Capture. Angew. Chem., Int. Ed. 2019, 58, 3885-3889. (k) Han, Y.; Meng, Z.; Ma, Y. X.; Chen, C. F. Iptycene-Derived Crown Ether Hosts for Molecular Recognition and Self-Assembly. Acc. Chem. Res. 2014, 47, 2026-2040.
- (18) (a) Guo, Q.-H.; Zhao, L.; Wang, M.-X. Synthesis and Molecular Recognition of Water-Soluble S_6 -Corona[3]arene[3]-pyridazines. *Angew. Chem., Int. Ed.* **2015**, *54*, 8386–8389. (b) Guo, Q.-H.; Zhao, L.; Wang, M.-X. Synthesis, Structure, and Molecular Recognition of S_6 -and $(SO_2)_6$ -Corona[6](het)arenes: Control of Macrocyclic Conformation and Properties by the Oxidation State of the Bridging Heteroatoms. *Chem. Eur. J.* **2016**, *22*, 6947–6955.
- (19) (a) Roberts, D. A.; Pilgrim, B. S.; Nitschke, J. R. Covalent Post-Assembly Modification in Metallosupramolecular Chemistry. *Chem. Soc. Rev.* **2018**, 47, 626–644. (b) Pilgrim, B. S.; Roberts, D. A.; Lohr, T. G.; Ronson, T. K.; Nitschke, J. R. Signal Transduction in a Covalent Post-Assembly Modification Cascade. *Nat. Chem.* **2017**, 9, 1276–1281.
- (20) $\mathbf{Ex''Box^{4+}}$ is a class of tetracationic cyclophane with a box-like geometry. The constitution of $\mathbf{Ex''Box^{4+}}$ is based on p-phenylene-bridged 4,4′-bipyridinium subunits, wherein two of these subunits are bridged by two p-xylylene linkers and n is the number of p-phenylene links between the two pyridinium units.
- (21) (a) Kaim, W. The Coordination Chemistry of 1,2,4,5-Tetrazines. *Coord. Chem. Rev.* **2002**, 230, 127–139. (b) Benson, C. R.; Hui, A. K.; Parimal, K.; Cook, B. J.; Chen, C. H.; Lord, R. L.; Flood, A. H.; Caulton, K. G. Multiplying the Electron Storage Capacity of a Bis-Tetrazine Pincer Ligand. *Dalton Trans.* **2014**, 43,

- 6513-6524. (c) Gao, W. X.; Feng, H. J.; Lin, Y. J.; Jin, G. X. Covalent Post-Assembly Modification Triggers Structural Transformations of Borromean Rings. *J. Am. Chem. Soc.* **2019**, *141*, 9160-9164.
- (22) For comparison, dimethyl-4-bptz 2·2PF₆ was also prepared as shown in Scheme 1.
- (23) All calculations were carried out at the B3LYP/6-31G* level in QChem 4.3. Geometry optimizations were performed without symmetry constraints. The molecular orbitals were generated with IQmol.
- (24) (a) Schottel, B. L.; Chifotides, H. T.; Dunbar, K. R. Anion-π Interactions. *Chem. Soc. Rev.* **2008**, *37*, 68–83. (b) Chifotides, H. T.; Dunbar, K. R. Anion-π Interactions in Supramolecular Architectures. *Acc. Chem. Res.* **2013**, *46*, 894–906. (c) Zhao, M.-Y.; Wang, D.-X.; Wang, M.-X. Synthesis, Structure, and Properties of Corona[6] arenes and Their Assembly with Anions in the Crystalline State. *J. Org. Chem.* **2018**, *83*, 1502–1509.
- (25) For examples of self-assembled superstructures stabilized by PF₆⁻ counterions, see: (a) Fyfe, M. C. T.; Glink, P. T.; Menzer, S.; Stoddart, J. F.; White, A. J. P.; Williams, D. J. Anion-Assisted Self-Assembly. *Angew. Chem., Int. Ed. Engl.* 1997, 36, 2068–2070. (b) Guo, Q.-H.; Liu, Z. C.; Li, P.; Shen, D. K.; Xu, Y. B.; Ryder, M. R.; Chen, H. Y.; Stern, C. L.; Malliakas, C. D.; Zhang, X.; Zhang, L.; Qiu, Y. Y.; Shi, Y.; Snurr, R. Q.; Philp, D.; Farha, O. K.; Stoddart, J. F. A Hierarchical Nanoporous Diamondoid Superstructure. *Chem.* 2019, 5, 2353–2364.
- (26) $CoCp_2$ was chosen as a chemical reductant for three reasons: (i) it is soluble in DMF and affords a homogeneous solution, (ii) it possesses a sufficiently negative reduction potential, allowing it to reduce $TzBox^{4+}$ to its neutral state, and (iii) it provides precise control over the number of equivalents of the reductant.
- (27) Waldhor, E.; Zulu, M. M.; Zalis, S.; Kaim, W. Coordination-Induced Switch Between the Singly Occupied and the Lowest Unoccupied Molecular Orbitals in Two Methylviologen-Derived Chromophores. J. Chem. Soc., Perkin Trans. 2 1996, 1197–1204.
- (28) (a) Trabolsi, A.; Khashab, N.; Fahrenbach, A. C.; Friedman, D. C.; Colvin, M. T.; Cotí, K. K.; Benítez, D.; Tkatchouk, E.; Olsen, J. C.; Belowich, M. E.; Carmielli, R.; Khatib, H. A.; Goddard, W. A., III; Wasielewski, M. R.; Stoddart, J. F. Radically Enhanced Molecular Recognition. *Nat. Chem.* **2010**, *2*, 42–49. (b) Frasconi, M.; Fernando, I. R.; Wu, Y.; Liu, Z.; Liu, W. G.; Dyar, S. M.; Barin, G.; Wasielewski, M. R.; Goddard, W. A., III; Stoddart, J. F. Redox Control of the Binding Modes of an Organic Receptor. *J. Am. Chem. Soc.* **2015**, *137*, 11057–11068.
- (29) The reduction of tetrazine to 1,4-dihydro-tetrazine and diaminoazine has been reported previously: (a) Schwach, M.; Hausen, H.-D.; Kaim, W. The First Crystal Structure of a Metal-Stabilized Tetrazine Anion Radical: Formation of a Dicopper Complex through Self-Assembly in a Comproportionation Reaction. *Inorg. Chem.* 1999, 38, 2242–2243. (b) Glockle, M.; Hubler, K.; Kummerer, H. J.; Denninger, G.; Kaim, W. Dicopper(I) Complexes with Reduced States of 3,6-Bis(2'-Pyrimidyl)-1,2,4,5-Tetrazine: Crystal Structures and Spectroscopic Properties of the Free Ligand, a Radical Species, and a Complex of the 1,4-Dihydro Form. *Inorg. Chem.* 2001, 40, 2263–2269.
- (30) The synthesis of $DzBox^{4+}$ has been reported previously: Fang, Q. S.; Chen, L.; Liu, Q. Y. Template-Directed Synthesis of Pyridazine-Containing Tetracationic Cyclophane for Construction of [2]-Rotaxane. *Chin. Chem. Lett.* **2017**, 28, 1013–1017.
- (31) As shown in Figure 5a, the height is defined as the centroid-to-centroid distance between the top and bottom planes of the box. The width is defined as the centroid-to-centroid distance between the planes of the two p-phenylene spacers. The length is defined as the centroid-to-centroid distance between the planes of the two p-xylylene rings linking the two pyridinium units.
- (32) $TzBox\cdot4PF_6$ and $DzBox\cdot4PF_6$ were chosen because of the ease of their synthees.
- (33) For other examples where anion— π interactions have been shown to modulate binding constants, see: Hafezi, N.; Holcroft, J. M.; Hartlieb, K. J.; Dale, E. J.; Vermeulen, N. A.; Stern, C. L.; Sarjeant, A.

A.; Stoddart, J. F. Modulating the Binding of Polycyclic Aromatic Hydrocarbons Inside a Hexacationic Cage by Anion– π Interactions. Angew. Chem., Int. Ed. **2015**, 54, 456–461.

(34) Single crystals were obtained by slow vapor diffusion of iPr₂O into MeCN solutions containing equimolar amounts of hosts and guests at room temperature.